ACCUMULATION and ANNEALING of RADIATION DONOR DEFECTS in ARSENIC-IMPLANTED $Hg_{0.7}Cd_{0.3}Te$ FILMS

R4-P-005201

The 7-th International Congress on Energy Fluxes and Radiation Effects (EFRE 2020)

19th International Conference on Radiation Physics and Chemistry of Condensed Matter

Tomsk, Russia. September 14-26, 2020

AUTORS

A.V. Voitsekhovskii[1], A.G. Korotaev[1]

[1]National Research Tomsk State University, Tomsk, Russia;

I.I. Izhnin[1,2]

[2]SRC "Electron-Carat", Lviv, Ukraine;

K.D. Mynbaev[3]

[3]Ioffe Institute, Saint-Petersburg, Russia;

V.S. Varavin[4], S.A. Dvoretsky[4], D.V. Marin[4], N.N. Mikhailov[4], M.V. Yakuszev[4]

[4]Rzhanov Institute of Semiconductor Physics, SB RAS, Novosibirsk, Russia.

O.I. Fitsych[5]

[5]P.Sagaidachny Army Academy, Lviv, Ukraine;

K.R. Kurbanov[6]

[6]Kremenchug Flight College, Kremenchug, Ukraine.

MOTIVATION

- For $Cd_xHg_{1-x}Te$ (MCT), the basic material for infrared photo–electronics, there are various configurations of *p-n* junctions of photodiodes; for their creation, ion implantation is usually used.
- The most promising design of *p–n* junctions used in photodiodes based on MCT, relies on fabrication of local *p*–type regions in an *n*–type base with the use of implantation of arsenic.
- Ion implantation, however, leads to the formation of various types of radiation donor defects, so to form a required *p*–type region one needs to anneal the defects and to activate the introduced arsenic atoms electrically.
- To perform an effective annealing, it is necessary to know the processes of accumulation and annealing of the radiation donor defects. However, to date such investigations have been made mainly in arsenic-implanted $Cd_xHg_{1-x}Te$ with x_a~0.22, which is material serving as a basis for the fabrication of long-wavelength infrared (IR) photodiodes.
- **The aim of this work was to study the processes of accumulation and annealing of the radiation donor defects in arsenic-implanted $Cd_xHg_{1-x}Te$ with x_a~0.3, the material suitable for the development of middle-wavelength IR detectors.**

EXPERIMENTAL DETAILS

- Un-doped films were grown by molecular-beam epitaxy (MBE) at the Rzhanov Institute of Semiconductor Physics (Novosibirsk, Russia) on (013) CdTe/ZnTe/GaAs (or Si) substrates; *in situ* ellipsometric measurements were used to monitor their composition and thickness. Their 'absorber' layer with uniform CdTe molar fraction (composition) x_a~0.3 was covered with a graded-gap protective layer (GPL) with composition at the surface x_s=0.46-0.6. The thickness of the GPL was ~0.2-0.4 μm.
- Electrical properties of the initial samples, samples after ion implantation (II) and II + annealing were investigated by measuring the field dependences of the Hall coefficient R_H (B) and the conductivity σ (B) in magnetic fields B = 0.01-1.5 T at 77 K and their analysis by the discrete mobility spectrum method (DMSA). This allowed us to determine the number of species and their parameters: concentration, mobility and partial conductivity.
- **Two type of films were investigated:**
- The studies of accumulation of radiation donor defects were performed on films with *p*–type conductivity (due to the presence of mercury vacancies, acceptors in MCT) Mi14 and Mi15 after As II with energies E=190 keV and E=350 keV and ion fluences ranging from 10^{12} to 10^{15} cm^{-2} without annealing:

Mi14 – $p=1.6\cdot10^{16}$ cm^{-3}, $\mu_p=290$ $cm^2/(V\cdot s)$; $\sigma_0=0.63$ $(\Omega\cdot cm)^{-1}$;

Mi15 – $p=1.9\cdot10^{16}$ cm^{-3}, $\mu_p=230$ $cm^2/(V\cdot s)$, $\sigma_0=0.72$ $(\Omega\cdot cm)^{-1}$.

The dependences of the concentration of radiation donor defects (the concentration of electrons with low mobility) on the ion fluence were analyzed and compared with those for samples with x_a = 0.22.

- The studies of annealing of radiation donor defects were performed on films with *n*–type conductivity (due to the presence of residual donors) Mi16 and Mi17 after As II with energies E=190 keV and E=350 keV and ion fluence 10^{14} after II and II + annealing:

Mi16 – $n=7.1\cdot10^{13}$ cm^{-3}, $\mu_n=49500$ $cm^2/(V\cdot s)$; $\sigma_0=0.68$ $(\Omega\cdot cm)^{-1}$;

Mi17 – $n=1.3\cdot10^{14}$ cm^{-3}, $\mu_p=42600$ $cm^2/(V\cdot s)$, $\sigma_0=1.18$ $(\Omega\cdot cm)^{-1}$.

The set of the carriers after II and II + annealing was analyzed and compared with that for samples with x_a = 0.22.

SET of CARRIERS in II *p*-TYPE SAMPLES

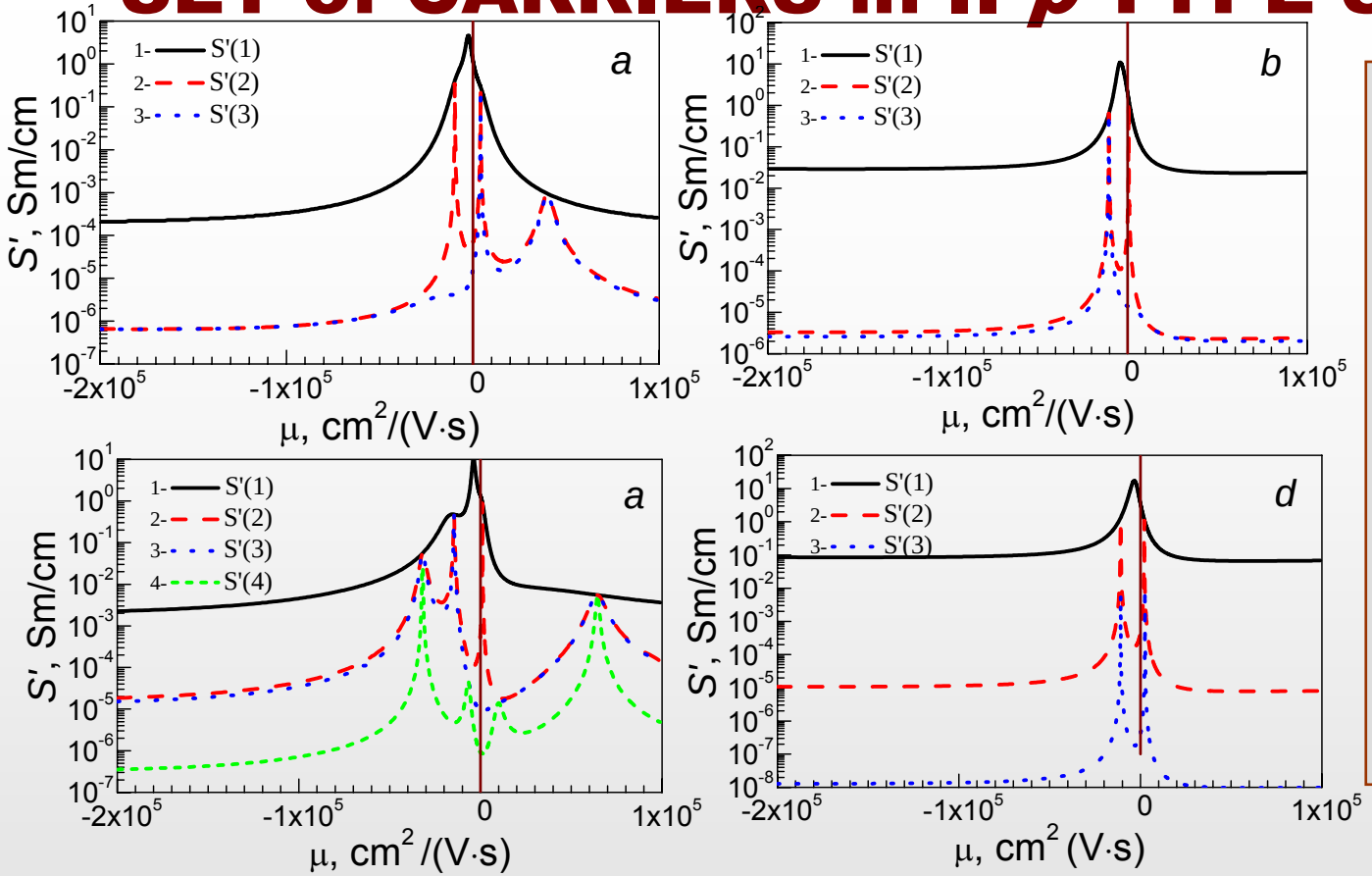

Fig. 1. Mobility spectra envelopes for investigated films Mi14-13 (a), Mi14-3 (b), Mi15-13 (c) and Mi15-3 (d) constructed for samples after ion implantation with fluence $\Phi=10^{13}$ cm^{-2} and energy E=190 keV (a, c) and E=350 keV (b, d): primary envelope (S1) and envelopes after two (a, b, d) or three (c) consecutive discretization steps (S2, S3 and S4, respectively

For sample Mi14 after II with *E*=190 and *E*=350 keV and sample Mi15 after II with *E*=350 keV for all fluences n^+–*p* structure was formed as a result of II. n^+-layer was formed by radiation donor defects represented by interstitial mercury Hg_I trapped by dislocation loops (producing low-mobility electrons (2500–4000 cm²/(V·s)) and quasi-point defects (producing mid-mobility electrons (10000–15000 cm²/(V·s)).

For sample Mi15 after II with *E*=190 keV for all fluences an n^+–*n*–*p* structure was formed, typical of arsenic-implanted films with x_a≈0.22. n-layer was formed by residual donor centers after annihilation of Hg_I with mercury vacancies.

The dominating contribution to the conductivity (80%) was that by the low-mobility electrons.

PRIMARY MOBILITY SPECTRUM ENVELOPES in *p*-TYPE FILMS

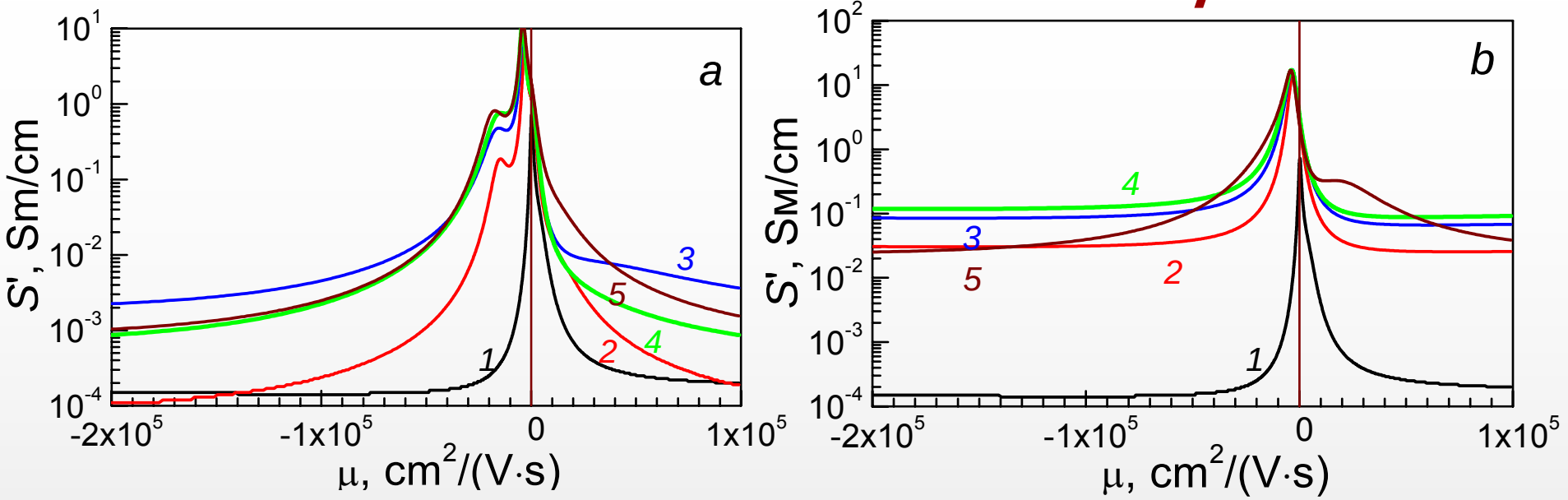

Fig. 2. Primary mobility spectrum envelopes for film M15 implanted with E=190 keV (a) and E=350 keV (b): 1, as-grown samples, and 2, 3, 4 and 5, samples implanted with fluences 10^{12}, 10^{13}, 10^{14}, and 10^{15} cm^{-2}, respectively.

Fig. 2 shows the transformation of envelopes for sample Mi15 implanted with *E*=190 keV and *E*=350 keV. The envelopes are clearly indicative of the dominating contribution to the conductivity by the low-mobility electrons (the strongest peak in the spectra near to zero mobility axis). For *E*=190 keV, with fluence increasing, the amplitude of the peak corresponding to the low-mobility electrons increased and showed no sign of saturation (Fig. 2a). For *E*=350 keV, the amplitude of the the low-mobility electrons peak changed insignificantly with fluence increasing (Fig. 2b). As the low-mobility electrons in II material originate in radiation-induced defects, the data were indicative of the saturation of the concentration of these defects.

ACCUMULATION of RADIATION DONOR DEFECTS

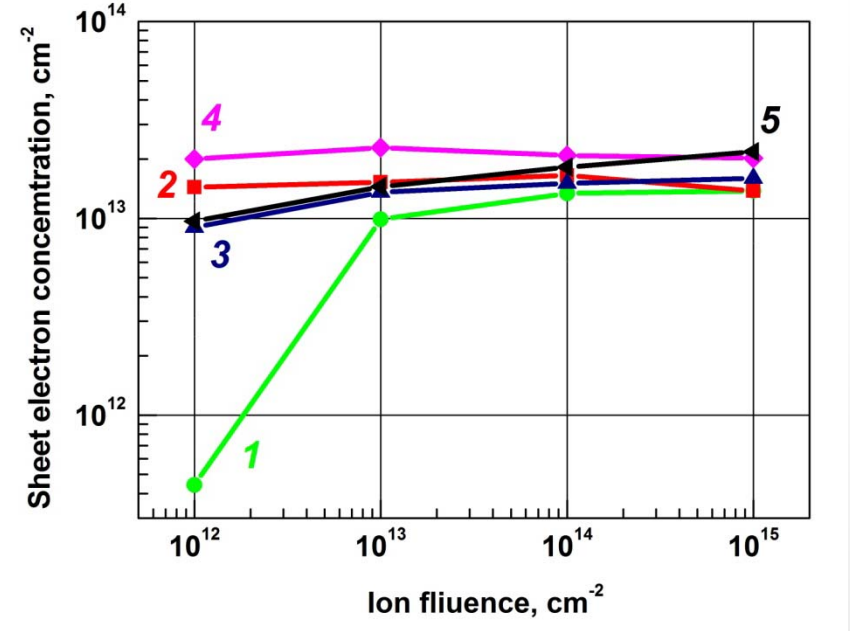

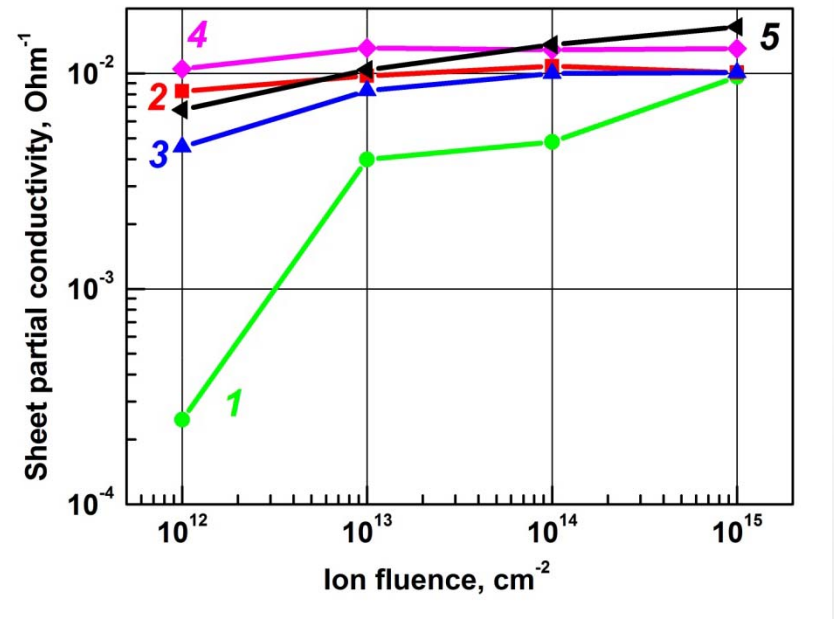

Fig.3. Fluence dependences of sheet concentration and partial conductivity provided by the low-mobility electrons in samples Mi14 (1, 2) and Mi15 (3, 4) implanted with E=190 keV (1, 3) and E=350 keV (2, 4), respectively. Data 5 show similar dependence for an MCT sample with x_a≈0.22 implanted with E=190 keV.

As follows from Fig. 3, for films with x_a≈0.30 the increase in the sheet electron concentration and partial conductivity with the fluence increasing was not that steep than that for films with x_a≈0.2. With the exception of sample Mi14 implanted with E=190 keV and fluence Φ=10^{12} cm^{-2}, the Ns and Σs in samples with x_a≈0.30 experienced saturation when fluences exceeded 10^{13} cm^{-2}. It is suggested that this difference was due to the effect of the built-in internal electric field of GSL. In films with x_a≈0.30 the value of the internal electric field would be smaller than that in samples with x_a≈0.22 with similar x_s, so the effect of this field on the dynamics of accumulation of implantation-induced defects should be weaker, too.

SET of CARRIERS in II and ANNEALED *n*-TYPE SAMPLES

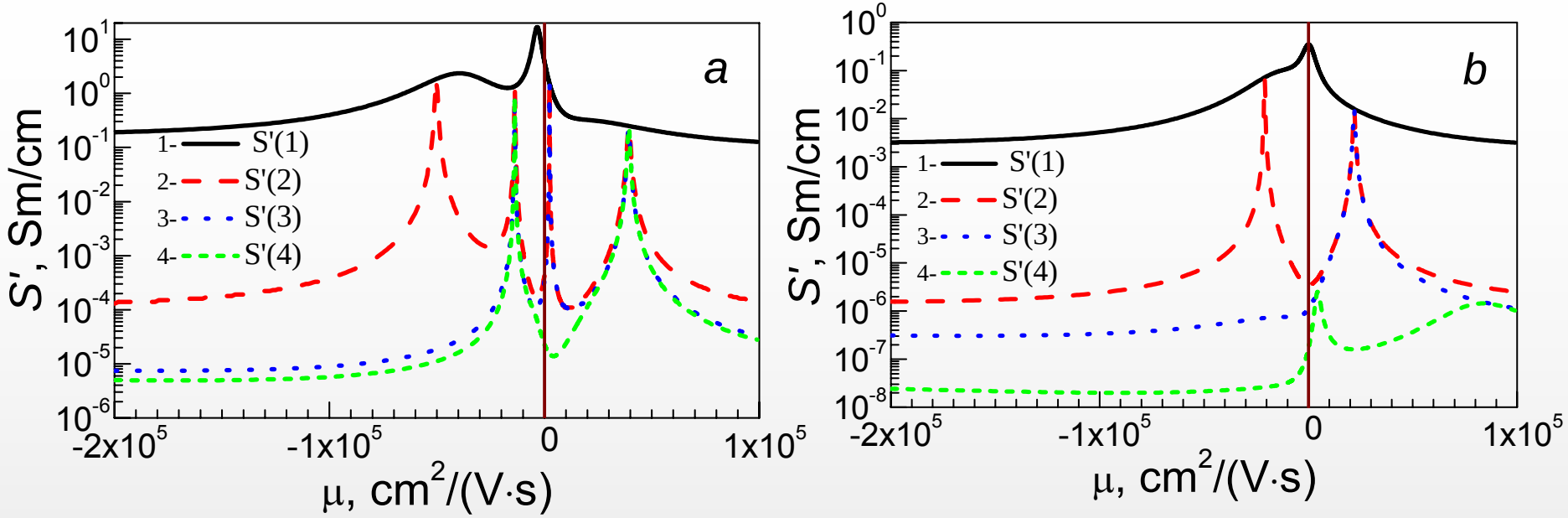

Fig. 4. Mobility spectra envelopes for films Mi17 after II with $\Phi=10^{14}$ cm^{-2} and E=350 keV (a), and for films Mi17 after II and activation annealing (b): primary envelope (S1) and envelopes after three consecutive discretization steps S2, S3 and S4, respectively.

For sample Mi17 after II with *E*=350 keV and $\Phi=10^{14}$ cm^{-2} fluences, the n^+–*n* structure was formed. The n^+-layer was formed by radiation donor defects producing low-mobility electrons (3300–4000 cm^2/(V·s) and mid-mobility electrons (14000–19000 cm^2/(V·s)). The *n*-layer with high mobility electrons represented the material that was not affected by the implantation. The dominating contribution to the conductivity (80%) was that by the low-mobility electrons.

For sample Mi17 after II and typical activation annealing (AA), a p^+–*n* structure was formed, were p^+– layer represents the layer with implanted and activated As, where conductivity was dominated by the heavy holes. The contribution to conductivity by the high-mobility electrons could not be detected at all. The degree of the electrical activation of arsenic after the annealing, though, appeared to be low, ~0.1

PRIMARY MOBILITY SPECTRUM ENVELOPES in *n*-TYPE FILMS

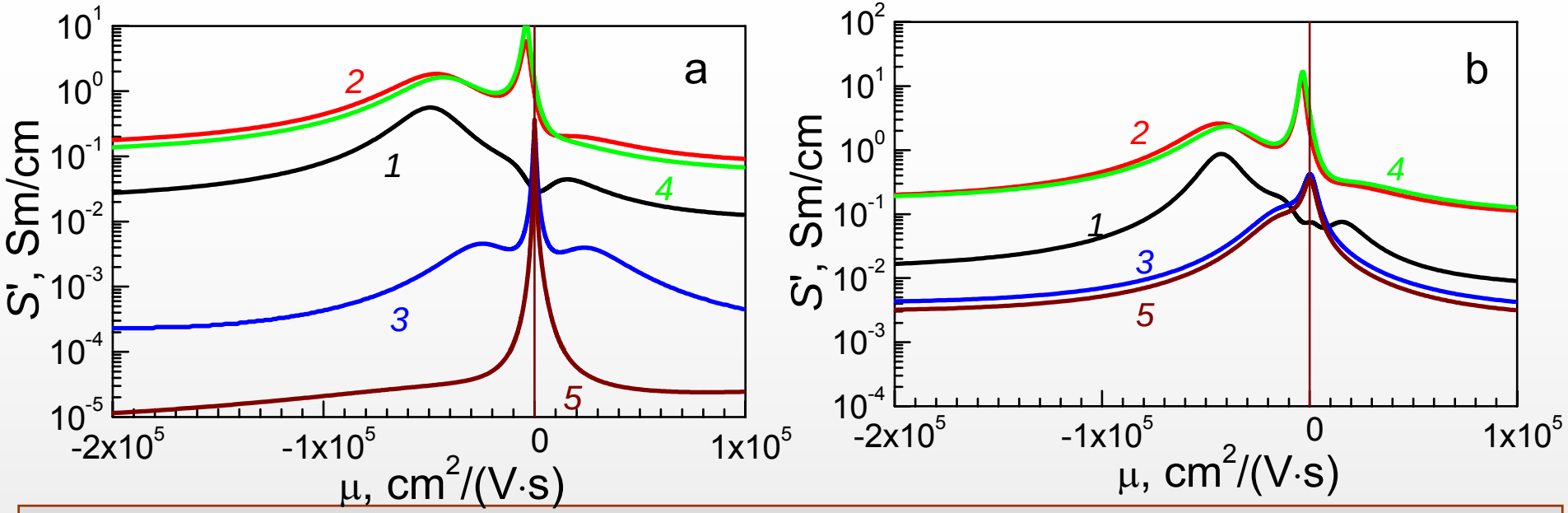

Fig. 5. Primary mobility spectra envelopes for films Mi16 (a) and Mi17 (b): 1, as-grown film; 2, after II with E=190 keV; 3, after AA of sample implanted with E=190 keV; 4, after II with E=350 keV; 5, after AA of sample implanted with E=350 keV.

Fig. 5 shows the transformation of the primary envelopes of the mobility spectra for *n*-type samples Mi16 and Mi17 II with fluence 10^{14} cm^{-2} at energies *E*=190 keV and *E*=350 keV and subjected to arsenic AA. In the as-grown sample, the major contribution to conductivity was that by the majority carriers of the 'active' layers, i.e., the high-mobility electrons (curve *1*). After the implantation, the conductivity was dominated by the low-mobility electrons originated in donor defects induced by implantation (curves *2* and *4*); still, high-mobility electrons were also present. After AA, the mobility peak due to the low-mobility electrons disappeared (curves *3* and *5*), which was indicative of the annihilation of the implantation-induced defects. At the same time, curves *3* and *5* demonstrated mobility peaks near the 'zero' mobility value. This was indicative of the appearance of hole mobility due to the electrical activation of the implanted arsenic ions.

CONCLUSION

- In our study of MBE-grown *p*-type HgCdTe films with $x_a \approx 0.30$ implanted with arsenic (and not annealed) we observed formation of 'n^+–p' structures or 'n^+–n–p' structures (typical of films with $x_a \approx 0.22$). The dominating (~80%) contribution to conductivity in the implanted samples was that by the low-mobility (2500-4000 $cm^2/(V \cdot s)$) electrons originated in donors possibly related to the interstitial mercury captured by the implantation-induced dislocation loops. The next, much lower, contribution was that by the mid-mobility (10000-15000 $cm^2/(V \cdot s)$) electrons originated in the interstitial mercury captured by the implantation-induced quasi-point defects.
- In contrast to samples with $x_a \approx 0.22$, in samples with $x_a \approx 0.30$ we observed weak dependences of concentration and partial conductivity provided by the low-mobility electrons on ion fluence; at 10^{13} cm^{-2} fluence, a saturation of the dependence was observed. It was suggested that this difference is caused by the different effect of the built-in electric field of graded-gap surface layer in samples with $x_a \approx 0.30$ and $x_a \approx 0.22$ with x_s being similar and equaling 0.45.
- The degree of the electrical activation of implanted arsenic as a result of the annealing in originally *n*-type samples with $x_a \approx 0.30$ appeared to be much lower than that in samples with $x_a \approx 0.22$. Also, in contrast to the latter, the annealing performed in this work did not result in the restoration of the electrical properties of the *n*-type 'base' of the photodiode structures. These effects may be related to the different impurity backgrounds in samples with $x_a \approx 0.30$ and $x_a \approx 0.22$ and requires further investigation.